Coordination Chemistry Reviews 254 (2010) 1419–1433

Contents lists available at ScienceDirect

Coordination Chemistry Reviews

journal homepage: www.elsevier.com/locate/ccr

Review

Interactions modes and physical properties in transition metal chalcogenolene-based molecular materials

Maria Laura Mercuri*, Paola Deplano, Luca Pilia, Angela Serpe, Flavia Artizzu**

Università di Cagliari, Dipartimento di Chimica Inorganica e Analitica, S.S. 554 – bivio per Sestu –I-09042-Monserrato (CA), Italy

Contents

ARTICLE INFO

Article history:
Received 5 August 2009
Accepted 7 October 2009
Available online 20 October 2009

Keywords:
Metal dithiolenes
van der Waals interactions
H-bonding
π–d Interaction
Single-component molecular metals
Multifunctional materials

ABSTRACT

Molecule-based materials are extremely versatile materials as they can be built from specifically designed building blocks with the desired size, shape, charge and electronic properties which determine their intermolecular interactions and, thus, their organization in the solid. The intermolecular interactions, therefore, in particular van der Waals interactions, π–π and π–d interactions, H-bonding, *etc.*, play a crucial role in self-assembling these pre-designed molecular units and may provide a powerful way to afford layered mono- and multifunctional molecular materials with new or unknown physical properties. In this review the relationship between interaction modes and physical properties of organic/inorganic hybrids based on transition metal complexes with chalcogenolene ligands will be examined and an outlook will be proposed. With this goal, magnetic materials, highly conducting and metallic single-component materials containing dithiolene complex building blocks, multifunctional materials where the dithiolene complex is the magnetic or conducting component in addition to more complex systems involving other types of building block such as the metal oxalate complexes, will be discussed.

1. Introduction

Interest in molecule-based materials, namely materials built from pre-designed molecular building blocks, is increased in recent years, since they are known to exhibit many technologically important properties (e.g., magnetic ordering, electrical conductivity, superconductivity, and ferroelectricity) traditionally considered to be solely available for classic atom-based inorganic solids such as metals, alloys or oxides. Molecular materials are obtained through soft routes, traditionally from organic chemistry, coordination chemistry and supramolecular chemistry and this opens unprecedented possibilities to the design of molecules with the desired size, shape, charge, polarity, and electronic properties. Intermolecular interactions play a crucial role in assembling these molecular bricks into one-, two- and three-dimensional arrays with a desired structure and functionality. These interactions can go from hydrogen bonding and cation–anion electrostatic interactions, to dipole–dipole or van der Waals interactions, including any combination of them; the strength and directionality of all of them determine the supramolecular structure of materials and their physical properties. Representative examples of molecule-based materials which have been synthesized up to know are: (i) highly conducting and metallic single-component materials; (ii) magnetic

* Corresponding author. Tel.: +39 070 6754486; fax: +39 070 6754456.
** Corresponding author.
E-mail addresses: mercuri@unica.it (M.L. Mercuri), f.artizzu@unica.it (F. Artizzu).

0010-8545/$ – see front matter © 2009 Elsevier B.V. All rights reserved.
doi:10.1016/j.ccr.2009.10.002

materials such as ferromagnets, ferrimagnets, metamagnets and spin ladders (molecular systems consisting of assemblies of $S = 1/2$ chains, one next to the other) in addition to other systems suitable for the study of magnetic ordering and (iii) multifunctional hybrids formed by the combination of two different molecules, a cationic species and an anionic species, which have a strong tendency to self-assemble through cation–anion electrostatic interactions forming two-network materials where two different physical properties coexist or even interplay.

Sulfur-rich planar π-conjugated molecules such as tetrathiafulvalene (TTF) and metal dithiolenes are useful redox-active building blocks for the design and synthesis of molecular conductors, magnets and conducting/magnetic organic/inorganic hybrids owing to their open-shell electronic structure and strong intermolecular interactions through S···S contacts. The field of molecular conductors started with the synthesis of the first organic one-dimensional (1D) molecular metal (TTF)(TCNQ) (TCNQ = tetracyanoquinodimethane) [1] showing a metallic state down to 55 K and the discovery of superconductivity in $(TMTSF)_2PF_6$ (TMTSF = tetramethyltetraselenofulvalene)[1] [2], formed by a two-dimensional (2D) network due to short Se···Se contacts between the TMTSF stacks. In 1986 the first molecular superconductor containing a metal dithiolene complex [TTF][Ni(dmit)$_2$]$_2$ [3], with Tc = 1.6 K under $P = 7$ kB was synthesized and subsequently superconductivity (Tc = 1.3 K) at ambient pressure was discovered in α-(EDT-TTF)[Ni(dmit)$_2$] (EDT-TTF = ethylenedithio-tetrathiafulvalene) [4]. Although in terms of molecular architecture the M(dmit)$_2$ complex, where the central electron-delocalized core is extended by the sulfur-containing heterorings (Chart 1), is similar to the BEDT-TTF molecule, the transverse interactions were found to be weaker than expected and unable to realize a 2D network and the superconductivity was only stabilized at very low temperatures. Thus the M(dmit)$_2$ (M = Ni, Pd) superconductors [5] occupy a unique position because almost all molecular superconductors were formed by organic molecules having TTF-like skeletons. Metal dithiolenes were also versatile bricks for building bulk ferromagnets and magnetic molecular conductors. $[NH_4][Ni(mnt)_2]\cdot H_2O$ [6], formed by uniform stacks of planar [Ni(mnt)$_2$] complexes separated by ammonium cations (which favour the uniform stacking because of their small size), is an insulator showing antiferromagnetic interactions at $T > 100$ K, ferromagnetic coupling below this temperature and ferromagnetic ordering at $T < 5$ K; (Cp_2^*Mn)[Ni(mnt)$_2$] ($Cp^* = \eta^5$-pentamethylcyclopentadienyl) [7], which consists of ···D$^+$D$^+$A$^-$A$^-$D$^+$D$^+$A$^-$A$^-$··· stacks formed by side-by-side cations alternating with dyads, is a semiconductor showing ferromagnetic ordering at $T < 2.5$ K. The (per)$_2$M(mnt)$_2$ (M = Fe, Co, Ni, Pd, Pt, Cu, Au; per = perylene) [8] represented the first family of paramagnetic molecular metals. In these compounds, M(mnt)$_2$ complexes form chains of localized spin units while the conducting properties are due to segregated perylene stacks. α-(per)$_2$M(mnt)$_2$ phases have a similar structure, with segregated stacks of perylene and M(mnt)$_2$ units along the stacking *b*-axis. They show high room-temperature conductivity along the stacking axis ranging from 700 S cm^{-1} for the M = Ni, Pt, Cu, Au compounds to 300 S cm^{-1} for the M = Pd, and 200 S cm^{-1} for the M = Fe and Co compounds while the magnetic behaviour strongly depends on the metal. Unfortunately the major problem associated with dithiolene complexes is their instability at low temperature due to metal-to-insulator (MI) transition caused by Peierls-type dimerizations along the chains [9]; these compounds usually crystallize forming stacks of complexes which give rise to quasi-1D electronic systems, thus preventing the occurrence of either the metallic state or superconductivity. The Peierls distortion may be suppressed at low temperature by increasing the dimensionality of the systems either increasing the number of peripheral sulfur atoms in the ligand framework, in order to favour lateral S···S interactions, or changing from sulfur to selenium ligand analogues; the Se 4d orbitals have larger electron cloud diameters compared to the S 3d orbitals which can lead to an enhancement of the interaction in the complexes leading to an increase of both the dimensionality and the electrical conductivity of the systems [10,11]. Important milestones in the area of molecular magnetic conductors were also achieved using as building blocks the BEDT-TTF organic molecule or its selenium derivatives and charge-compensating anions ranging from simple mononuclear complexes $[MX_4]^{n-}$ ($M = Fe^{III}$, Cu^{II}; X = Cl, Br) and $[M(ox)_3]^{3-}$ (ox = oxalate = $C_2O_4^{2}$) with tetrahedral and octahedral geometry to layered structures such as the bimetallic oxalate complexes $[M^{II}M^{III}(ox)_3]^-$ (M^{II} = Mn, Co, Ni, Fe, Cu; M^{III} = Fe, Cr). Three representative hybrid materials have been synthesized up to now: paramagnetic/superconductor $(ET)_4[H_3OM^{III}(C_2O_4)_3]\cdot S$ (M^{III} = Cr, Fe and Ga; S = C_6H_5CN, $C_6H_5NO_2$, PhF, PhBr, *etc.*) [12a–e]; antiferromagnetic/superconductor κ-$(BETS)_2[FeBr_4]$ [13] and ferromagnetic/metal, the (BEDT-TTF)$_3$[MnCr(ox)$_3$] [14] being the most recent and significant advance in this field. As far as we know tris-chelated metal complexes with octahedral geometry are the most successful counterions for favouring the metallic state because of their capability to segregate the stacks compared to square-planar complexes such as d8 metal dithiolenes which favour instead alternate stacks and thus semiconducting or insulating state. In addition they have the possibility of a specific assembly order of Λ and Δ chirality that may influence the packing and thus the physical properties of the material as well as to introduce functionalities such as magnetic properties through both the metal and a suitably tailored ligand.

Because of the great diversity of metals, ligands, structures and physical properties, it is difficult to present a unified picture of what has been accomplished so far. The main results achieved in the field of molecule-based materials formed by the following molecular bricks (see Chart 1) have been reviewed by several authors.

Cassoux and Faulmann [5] and Robertson and Cronin [15], separately, reported on M(dmit)$_2$ and isologs, M(mnt)$_2$, M(dddt)$_2$ systems; Kato [16] analyzed the electronic structure of some of these systems, especially M(dmit)$_2$, by discussing geometrical aspects such as dimensionality, dimerization and frustration as well as the pressure effect on crystal and electronic structures and on the metallic and superconducting states. Kobayashi and coworkers [17] reported on single-component molecular metals with extended-TTF dithiolate ligands. Coronado and Day [18] discussed on the transport properties of magnetic molecular conductors formed by TTF derivatives (especially BEDT-TTF) and tetrahalometalate, trisoxalatometalate (III) anions, polyoxometalate clusters and chain anions such as M(mnt)$_2$ dithiolenes; recently Coronado and Galán-Mascarós [19] reviewed all aspects of the molecular ferromagnetic conductors built from the combination, in a single compound, of organic cationic radicals, able to give rise to conducting architectures, with polymeric anionic metal complexes, able to give rise to ferromagnetism.

The aim of the present work is not to complement the cited reviews but to highlight the role of the intermolecular interactions such as van der Waals, π–π, π–d, and H-bonding in determining the crystal packing and the physical properties of these molecular materials. Selected examples of conducting, magnetic and conducting/magnetic hybrids based on chalcogenolene transition metal complexes, whose structural features or physical properties are unusual with respect to analogous compounds reported in the literature up to now, will be discussed herein. In this context the molecular approach play a key role since it enables the

[1] *Cation radical salt* formed by anions with a well-defined charge state and radical cations of the TTF-type.

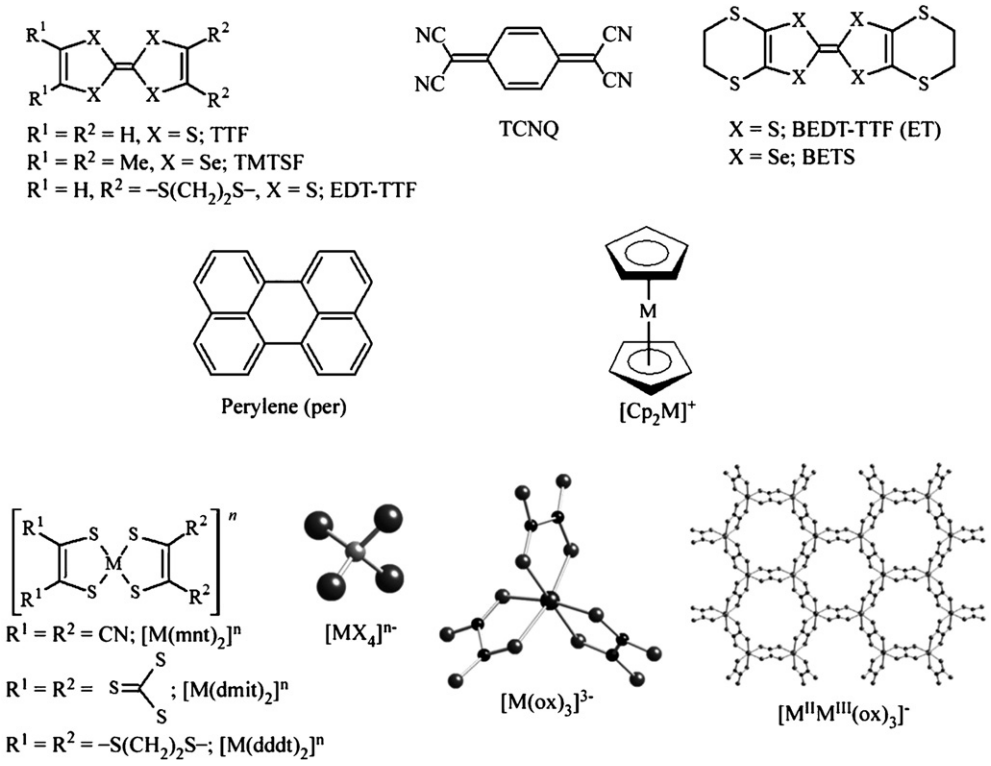

Chart 1.

chemical design of the molecular building blocks being suitable for self-assembly to form supramolecular structures with the desired interactions and physical properties.

2. van der Waals and π–π interactions

2.1. $[Ni(L)_2]^-$-based magnetic materials (L = dmit, tdas)

A variety of magnetic molecular materials have been prepared using the redox-active $[M(dmit)_2]$ molecular bricks which can serve as a source of localized $S = 1/2$ spins, depending on the metal oxidation state. Among them, materials based on the monovalent $[Ni(dmit)_2]^-$ (**11**) anion, bearing $S = 1/2$ spin, have shown various magnetic properties which arise from diverse modes of intermolecular interactions [5] and thus are of special interest in this context. The magnetic coupling in fact can be tuned by controlling the anisotropic intermolecular interactions. As shown in Fig. 1, the one, two, and three-dimensional magnetic exchange pathways within the crystals are defined by the following arrangements between the $[Ni(dmit)_2]^-$ anions: (a) π-stacking, (b and c) lateral S···S contacts along the long or short axes, and (d) the orthogonal π-overlap.

Supramolecular cations formed by inorganic or organic cations and crown ether derivatives have been shown to induce diverse $[Ni(dmit)_2]^-$ anion arrangements, depending on their size and shape, and long-range antiferromagnetic spin coupling has been observed for the majority of these compounds. Akutagawa and coworkers [20] have shown that symmetrical supramolecular cations such as (K^+)([18]crown-6), Ca^{2+}([18]crown-6)$(CH_3CN)_2$, and Cs^+_2([18]crown-6)$_3$, with a *C*3-axis through the center of the crown ether, normal to the molecular plane, form linear 1D $[Ni(dmit)_2]^-$ chain *via* lateral S···S interactions along the long axis, or π-dimers between the $[Ni(dmit)_2]^-$ anions which are antiferromagnetic arrangements of the $[Ni(dmit)_2]^-$ anion. Ferromagnetic interactions between the $[Ni(dmit)_2]^-$ anions may occur by reducing the symmetry of the supramolecular cation. In fact by using sandwich-type asymmetrical Cs^+_2(B[18]crown-6)$_3$ and Cs^+(DB[18]crown-6)$_2$ supramolecular cations, obtained by complexation with Cs^+ ions of benzo[18]crown-6 (B[18]crown-6) or dibenzo[18]crown-6 (DB[18]crown-6) crown ethers (see Scheme 1), unique arrangements of the $[Ni(dmit)_2]^-$ anions and consequently unique magnetic properties were observed in the Cs^+_2(B[18]crown-6)$_3[Ni(dmit)_2]^{-2}$ (**1**) and Cs^+(DB[18]crown-6)$_2[Ni(dmit)_2]^-$ (**2**) corresponding salts.

The crystal structures of both salts consisted of alternating layers of supramolecular cations and anions. In salt **1**, coexistence of a two-dimensional layer *via* lateral S···S contacts between the $[Ni(dmit)_2]^-$ anions (**A** and **B**) and a π-dimer chain of the anions (**C**) was observed (see Fig. 2).

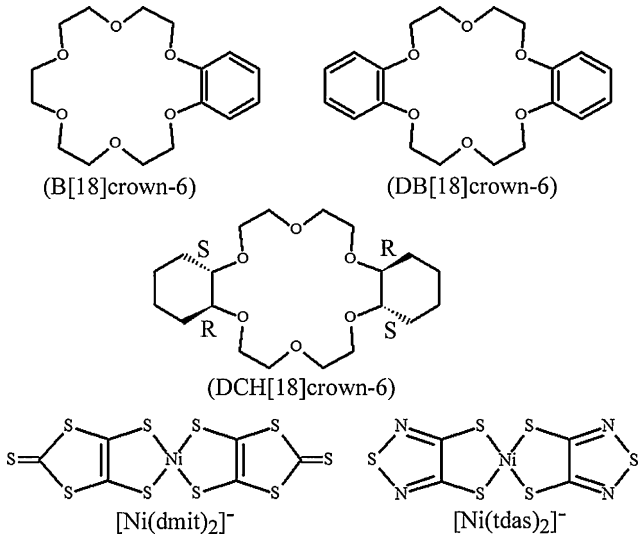

Scheme 1.

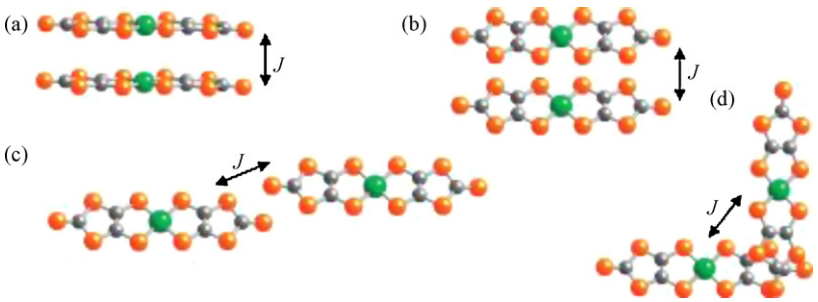

Fig. 1. Intermolecular interaction modes between the $[Ni(dmit)_2]^-$ anions: (a) π-dimer, (b) lateral S···S interactions along the short axis of the $[Ni(dmit)_2]^-$ anions, (c) lateral S···S interactions along the long axis of the $[Ni(dmit)_2]^-$ anions, and (d) orthogonal π-overlap. Reprinted with permission from Ref. [20]. Copyright 2009 American Chemical Society.

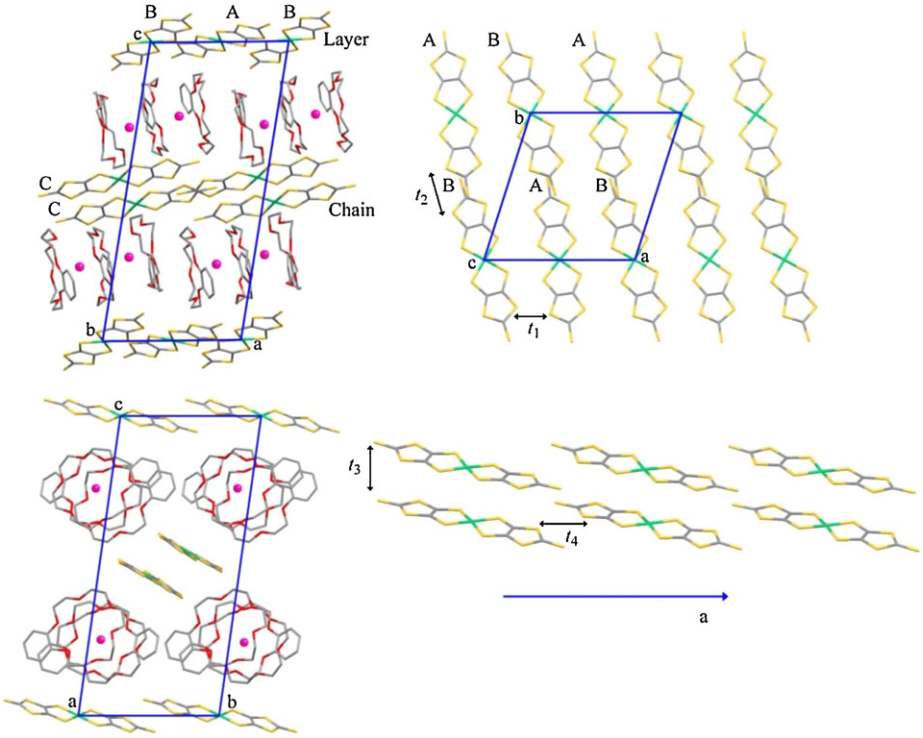

Fig. 2. Crystal structures of salt **1**. Unit cell viewed along the *b*-axis (a) and *a*-axis (b). Arrangements of the $[Ni(dmit)_2]^-$ anions in the two-dimensional **A**···**B** layer (c) and one-dimensional π-dimer chain of **C** (d). Intermolecular transfer integrals (*t*1–*t*4) are illustrated. Adapted with permission from Ref. [20]. Copyright 2009 American Chemical Society.

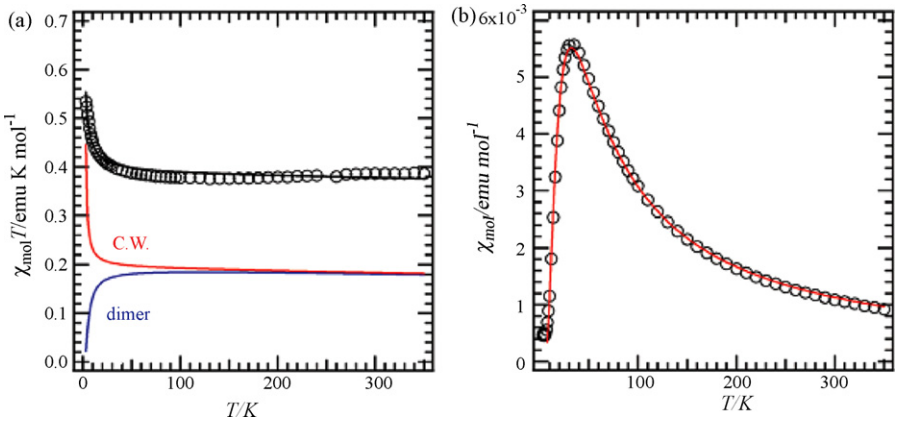

Fig. 3. Temperature-dependent molar magnetic susceptibility (χ_{mol}) of salts **1** and **2** per one $[Ni(dmit)_2]^-$ anion. (a) The χ_{mol} *T* vs. *T* plots of salt **1**. The χ_{mol} *T* was divided into the two components of the Curie–Weiss model with a positive *J*/*F* (red line) and a dimer model (blue line). The combination of both models is indicated as the black line in the χ_{mol} *T* vs. *T* plots. (b) The χ_{mol} *T* vs. *T* plots of salt **2**. Best fit using the dimer model (red line). Adapted with permission from Ref. [20]. Copyright 2009 American Chemical Society.

The magnetic properties of the π-dimer chain and the two-dimensional layer were characterized by antiferromagnetic ($J = -5.2$ K) and ferromagnetic coupling (Weiss temperature = +1.1 K), respectively. Transfer integrals based on extended Hückel molecular orbital calculations were used to evaluate the magnitude of the intermolecular interactions between $[Ni(dmit)_2]^-$ anions [21]. The unique $[Ni(dmit)_2]^-$ arrangements and magnetic behaviours of **1**, where ferromagnetic and antiferromagnetic coupling was shown to coexist (Fig. 3), can be attributed to the asymmetrical benzo[18]crown-6. In the case of salt (**2**), however, the formation of the lateral $[Ni(dmit)_2]^-$ dimer *via* S···S contacts yielded antiferromagnetic coupling corresponding to the dimer model ($J = -25.5$ K).

1D $[Ni(dmit)_2]^-$ lateral interactions *via* S···S contacts were also observed in the $(Ph\text{-}NH_3^+)(DCH[18]crown\text{-}6)[Ni(dmit)_2]^-$ (**3**) salt, a peculiar supramolecular rotator (molecular brick for building molecular machines) formed by assembling *via* H-bonding the anilinium ($Ph\text{-}NH_3^+$) cation and the bulky crown ether *meso*-dicyclohexano[18]crown-6 (DCH[18]crown-6) [21]. In this compound the $[Ni(dmit)_2]^-$ anions formed a uniform lateral S···S chain along the short axis of the $[Ni(dmit)_2]^-$ anions, as shown in Fig. 1b, in contrast to the π-stacking (Fig. 1a) and uniform lateral S···S chain along the long axis of $[Ni(dmit)_2]^-$ anions (Fig. 1c) modes, which yield to antiferromagnetic interactions. The magnetic behaviour, therefore, was dictated by the arrangement of the $[Ni(dmit)_2]^-$ anions which shows ferromagnetic coupling with a Weiss temperature = +0.9 K at low temperatures ($T < 30$ K). 1D lateral interactions *via* S···N contacts were observed in the (BEDT-TTF)$[Ni(tdas)_2]$ (**4**) [22] (tdas = 1,2,5-thiadiazole-3,4-dithiolate)[2], which represents the first example of a salt containing monomeric $[Ni(tdas)_2]^-$ monoanions. This salt forms a layered structure: one layer contains dimerized BEDT-TTF molecules and isolated $[Ni(tdas)_2]^-$ monoanions (**A**-type anions), while the second layer contains chains of $[Ni(tdas)_2]^-$ monoanions (**B**-type anions). According to the structure, the susceptibility data were fitted by a regular $S = 1/2$ antiferromagnetic chain (formed by the **B**-type anions) plus a monomeric contribution coming from the **A**-type anions. The antiferromagnetic intermolecular coupling between the **B**-type $[Ni(tdas)_2]^-$ units suggests that, although small, there is a nonnegligible interaction between these anions, in agreement with the presence of short interanion S–N distances (S23···N21 = 3.265(5)) observed in the crystal structure (see Fig. 4). The BEDT-TTF sublattice does not contribute to the magnetic properties as it consists of strongly antiferromagnetically coupled $(BEDT\text{-}TTF)_2^{2+}$ dimers as shown by the EPR spectra, magnetic susceptibility measurements, diffuse reflectance, and vibrational spectroscopy. This salt shows a semiconductor–semiconductor transition at about 200 K that may be attributed to an ordering of the disordered terminal ethylene group of the BEDT-TTF molecule.

2.2. $[Ni(\alpha\text{-}tpdt)_2]^{\bullet -}$-based magnetic materials

Previous studies with other dithiolene complexes [23] have shown that substituted benzopyridine cations favours segregated stacking of cations and anions leading to different kinds of magnetic interactions and ordering which depend on the overlap modes of the anions in the crystal structure. These cations in combination with the paramagnetic $[Ni(\alpha\text{-}tpdt)_2]^-$ (α-tpdt = 3,4-thiophenedithiolate) anionic dithiolene complex have produced

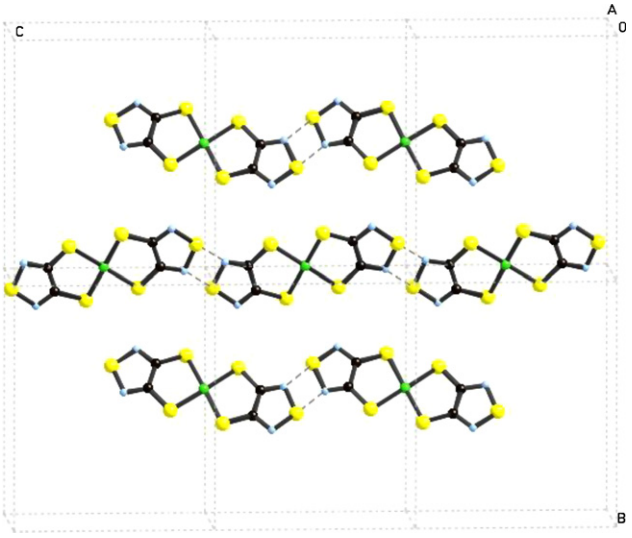

Fig. 4. View of the $[Ni(tdas)_2]^-$ **B** anionic layer down the *a*-axis. Thermal ellipsoids are drawn at the 20% probability level. Dashed lines indicate the intermolecular contacts shorter than the sum of the van der Waals radii. Adapted with permission from Ref. [22]. Copyright 2004 American Chemical Society.

three new salts (RBzPy)$[Ni(\alpha\text{-}tpdt)_2]$ (R = H, Br, F) (**5a**, **b**, **c**) [24]. The structure of all compounds consists of alternated layers of anions and cations: the anions are arranged with thiophenic sulfur atoms connecting to a coordinating sulfur atom of a neighbouring anion, placing the complexes almost perpendicular to their next neighbours, in zigzag chains. The cations are positioned with the pyridine rings inserted between thiophenic rings of anions, maximizing π–π interactions but failing in promoting segregated anion stacking. There are several anion–cation interactions: C···C and C···S π–π interactions between the pyridine ring of the cations and the thiophenic ring of the anions, S···H–C hydrogen bonds, C–Br···S short contacts through a coordinating and thiophenic sulfur atom and C–F···S interactions between anions and cations which are responsible for the prevalence of the *cis* configuration, never observed so far in a $[Ni(\alpha\text{-}tpdt)_2]^{\bullet -}$ dithiolene complex (Fig. 5).

The cation substitution plays a role in determining structural differences and variable amounts of *cis–trans* disorder in the anionic dithiolene complexes, related to the relative positions of the sulfur atoms of the thiophene rings. The *cis–trans* disorder affects the magnetic behaviour of these compounds: (HBzPy)$[Ni(\alpha\text{-}tpdt)_2]$ (**5a**) shows dominant ferromagnetic interactions and, at low temperatures, typical behaviour of a cluster glass as a consequence of disorder effects as shown in Fig. 6; (BrBzPy)$[Ni(\alpha\text{-}tpdt)_2]$ (**5b**) shows dominant antiferromagnetic interactions with a magnetic anomaly at $T \approx 6$ K and (FBzPy)$[Ni(\alpha\text{-}tpdt)_2]$ (**5c**) behaves like a paramagnet down to 1.5 K. This class of compounds shows how small changes within the building blocks can significantly affect the supramolecular interactions and thus the magnetic properties of the molecular material.

2.3. Conducting dithiolenes containing a TTF moiety

As already discussed in the Introduction, the $M(dmit)_2$ (M = Ni, Pd) superconductors [5] occupy a unique position because almost all molecular superconductors were formed by organic π molecules having TTF-like skeletons. Square-planar neutral metal bisdithiolene complexes were also found to be capable of showing high electrical conductivity, leading to a new type of molecular metals based on neutral species, the so-called single-component molecu-

[2] Metal complexes of the tdas ligand [22 and references therein] were proposed one decade ago as potential analogues of the $[M(dmit)_2]$ systems, but much easier obtainable in a one-step reaction from commercial precursors than the dmit-based complexes.

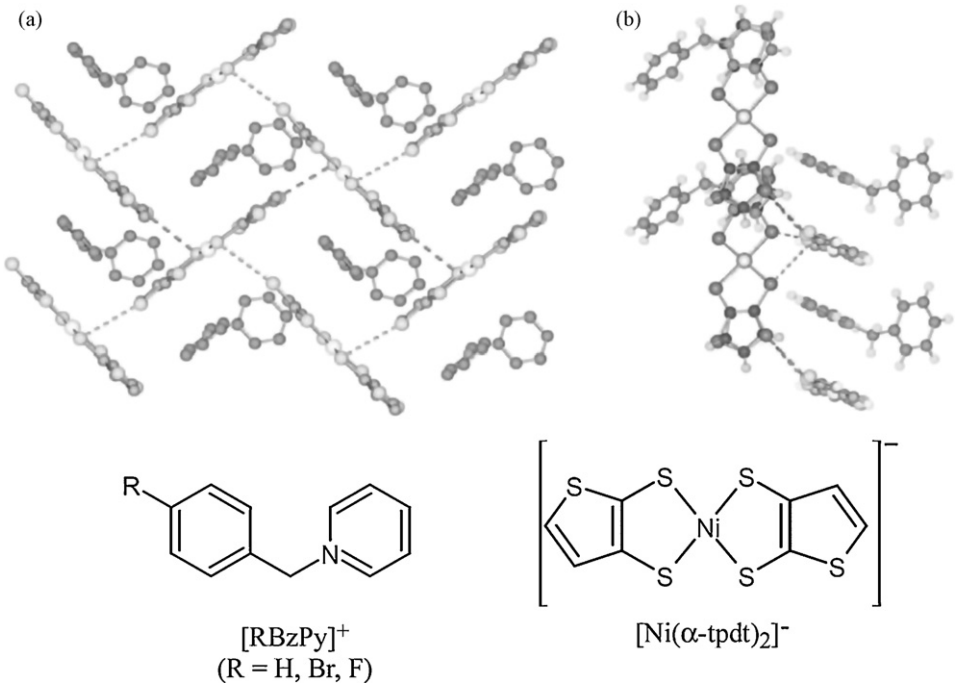

Fig. 5. Detail of the crystal structure of **5a**: (a) view perpendicular to one anionic layer with cations inserted in the layer and (b) detail showing the short contacts between anions in adjacent layers and the overlapping mode with anions. Reprinted with permission from Ref. [24]. Copyright 2006 Royal Society of Chemistry.

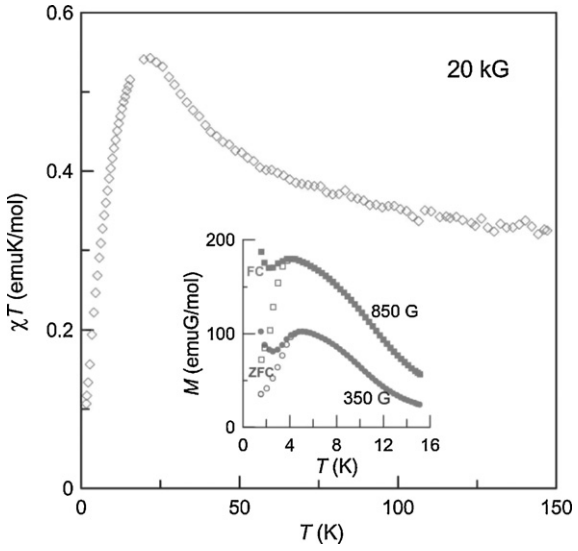

Fig. 6. Temperature dependence of χT for compound **5a**, under an applied field of 20 kG. The inset shows the ZFC (open symbols) and FC (closed symbols) magnetization curves for applied fields of 350 and 850 G, represented by circles and squares, respectively. Reprinted with permission from Ref. [24]. Copyright 2006 Royal Society of Chemistry.

lar metals (SCMMs).[3] To generate a metallic or semimetallic band in single-component molecules the energy separation between HOMO and LUMO should be small enough to make the HOMO and LUMO bands overlap each other through 2D or 3D van der Waals intermolecular interactions and to form partially filled bands. Therefore the molecules must have a very small HOMO–LUMO gap (ΔE) and large intermolecular interactions, especially transverse S···S contacts. Novel extended dithiolene ligands incorporating a TTF moiety were investigated since the first evidence of a very small ΔE from *ab initio* MO calculations on [Ni(ptdt)$_2$] (**6**) (ptdt = bis(propylenedithio)tetrathiafulvalenedithiolate) dithiolene complex [25]. The square-planar coordination geometry of metal bisdithiolenes is expected to favours π–π interactions while extended ligands are also expected to make more accessible different oxidation states. Theoretical calculations have shown that ΔE will tend to be small with increasing size on extended-TTF ligand system. Moreover the TTF-like structure is crucial for obtaining large transverse intermolecular interactions because the HOMO of the TTF-like donor has the same sign on every sulfur atoms and all intermolecular contacts through sulfur atoms enhance the intermolecular interaction by contributing additively [17]. Kobayashi and coworkers [26] have succeeded in preparing [Ni(tmdt)$_2$] (**7a**) (tmdt = trimethylenetetrathiafulvalenedithiolate) which exhibits a stable metallic state down to very low temperature (σ_{rt} = 400 S cm^{-1}, on single crystal) and several complexes based on dithiolene ligands containing TTF moieties, that often exhibit SCMM behaviour, such as [Cu(dmdt)$_2$] (**8**) (dmdt = dimethyltetrathiafulvalenedithiolate) [27], a SCMM incorporating magnetic moments and very recently [Au(tmdt)$_2$] (**7b**) [28], which is isostructural with [Ni(tmdt)$_2$] and highly conductive (50 S cm^{-1} at room temperature) down to 10 K. This single-component molecular conductor has been investigated by means of ^{1}H NMR for its unexpected magnetic behaviour. The spectral broadening and relaxation-rate enhancement at 110 K provide microscopic evidence that [Au(tmdt)$_2$] undergoes a magnetic phase transition at around 110 K, an extraordinarily high temperature among organic conductors (the quasi-two-dimensional system κ-(BEDT-TTF)$_2$Cu[N(CN)$_2$]Cl shows a T_N at around 27 K). As the susceptibility does not show a sudden increase below this temperature [29] the material cannot be ferromagnetic. The magnitude and temperature dependence of relaxation-rate indicates

[3] All molecular metals developed before 2000 were composed of two components: the molecules forming the electronic band (designated by A) and another chemical species (designated by B); the formation of a conduction band and the generation of charge carriers by the intermolecular charge-transfer between A and B seemed two essential requirements to ensure a metallic state in these systems [17].

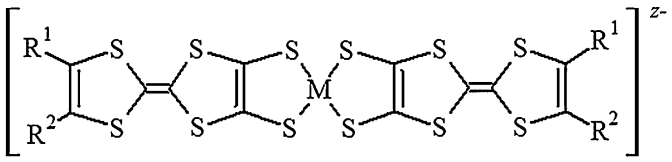

(6) $R^1 \wedge R^2 = -S(CH_2)_3S-$; $[M(ptdt)_2]^{z-}$

(7) $R^1 \wedge R^2 = -CH_2CH_2CH_2-$; $[M(tmdt)_2]^{z-}$, M=Ni (**a**), Au (**b**)

(8) $R^1 = R^2$ =Me; $[M(dmdt)_2]^{z-}$

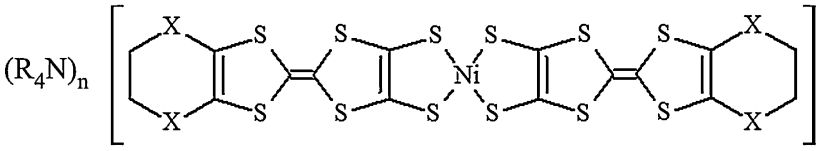

(9) **a** R = Me; X = CH_2; n = 2
b R = Bu; X = CH_2; n = 1
c X = CH_2; n = 0

(10) **a** R = Me; X = O; n = 2
b R = Bu; X = O; n = 1
c X = O; n = 0

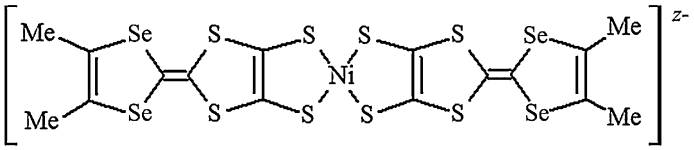

(11) $[Ni(dmstfdt)_2]^-$

Scheme 2.

that $[Au(tmdt)_2]$ is an unconventional metal with an antiferromagnetic order. It is well-known that low-dimensionality depresses a phase transition and causes spin contraction due to quantum fluctuations. $[Au(tmdt)_2]$ compound is a 3D system, as shown by the Fermi surface topology [30] and it is possible that three-dimensionality causes the high transition temperature and the large ordered moment [31].

New type of TTF-ligands fused with a six-membered rings such as cyclohexene and 1,4 dioxene which have structural flexibility such as the BEDT-TTF donor, have been used to obtain novel single-component highly conducting systems $(R_4N)_n[Ni(chdt)_2]$ [R = Me, n = 2 (**9a**); R = ^{n}Bu, n = 1 (**9b**); n = 0 (**9c**); chdt = cyclohexenotetrathiafulvalenedithiolate] and $(R_4N)_n[Ni(eodt)_2]$ [R = Me, n = 2 (**10a**); R = ^{n}Bu, n = 1 (**10b**); n = 0 (**10c**); eodt = ethylenedioxytetrathiafulvalenedithiolate] [32] (Scheme 2).

X-ray data were available only for **9b** and **10b** which show sandwiched structures in which the chains or layers of the nickel complexes and cations are arranged alternately. The anions form a 1D array along the *c*-axis and between adjacent anions there is one intermolecular S···S contact [3.646(1) Å] indicating side-by-side interactions along the *c*-axis. Interchain or interlayer S···S contacts less than the van der Waals radii were observed only in the transverse direction. The neutral species **9c** and **10c** showed large room-temperature conductivity (σ_{rt} = 1–10 S cm^{-1}) measured on pressed pellets of samples. Complex **10c** showed metallic temperature dependence down to 120 K and retained high conductivity down to 0.6 K, being thus considered a new single-component molecular metal. The magnetic behaviour of **9b** is in good agreement with the Bonner-Fisher model with $J/kB = -28$ K, showing the existence of an antiferromagnetic 1D Heisenberg chain [33] in agreement with the arrangement of anions with regular distance along the 1D chain (*c*-axis). Complex **10b** show Curie-Weiss paramagnetism with antiferromagnetic interactions between the S = 1/2 states.

Recently the new $(^nBu_4N)[Ni(dmstfdt)_2]$ (**11**) (dmstfdt = dimethyldiselenadithiafulvalenedithiolate; Scheme 2) Ni complex with STF (diselenadithiafulvalene)-type ligands has been synthesized and fully characterized [34]. This compound is a unique ambivalent molecular system exhibiting weakly metallic behaviour above room temperature and weak-ferromagnetism of localized spins at low temperature, despite the 1:1 stoichiometry similar to **9b** and **10b**. The crystallographically independent $[Ni(dmstfdt)_2]^-$ anions (A and B) are arranged along the stacking *a*-axis alternately and the dihedral angle of 42.6° between the molecular planes of adjacent anions produce a weakly dimerized zigzag array which form an anion layer parallel to the *ac*-plane. There are several intermolecular S···S(Se) contacts between the anions of the neighbouring zigzag arrays in addition to many contacts between the adjacent anions in the zigzag array, leading to a 2D network of intermolecular interactions in the anion layer (Fig. 7c).

Despite the 1:1 stoichiometry of the complex, the metallic behaviour is relevant. The room-temperature conductivity is σ_{rt} = 0.2 S cm^{-1} and metallic behaviour was observed down to 147 K at which temperature a sharp transition to an insulating state occurred. The temperature dependence of the magnetic susceptibility is also very unique, and the increase of the χT product vs. T suggest a localization of the conduction electrons with lowering temperature in the 160–280 K range, where the resistivity gradually increase. The χT value was constant in the 80–150 K range and this is fitted well by the Curie-Weiss law. $(^nBu_4N)[Ni(dmstfdt)_2]$ is a novel molecular metal which undergoes a transition to an insulat-

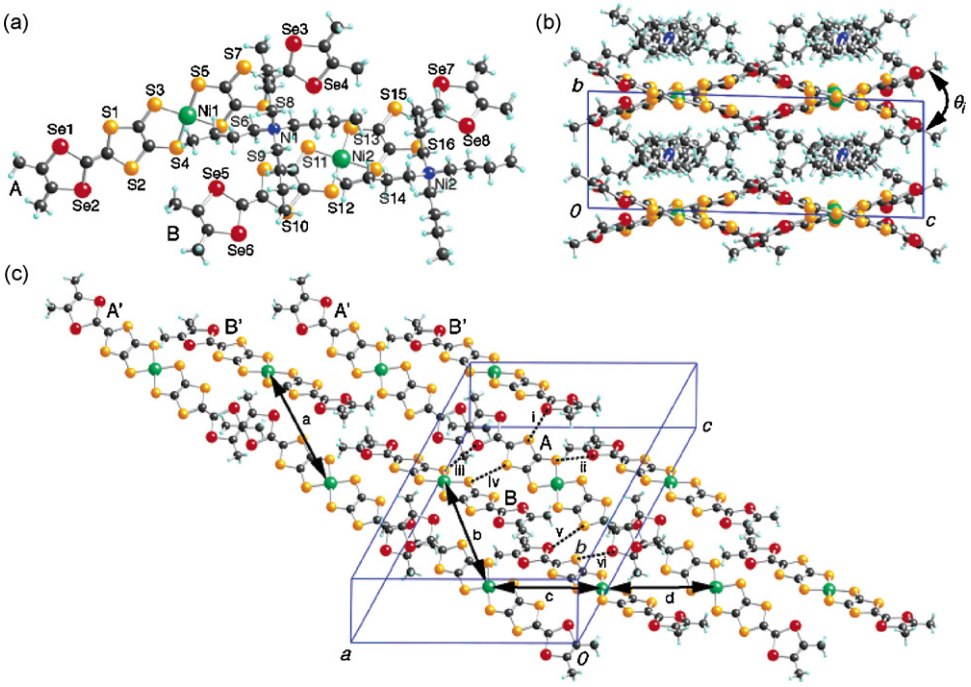

Fig. 7. Crystal structure of (^{n}Bu$_4$N)[Ni(dmstfdt)$_2$] (**11**) at room temperature. (a) Crystallographically independent molecules with labeling of the atoms. (b) Sandwiched structure of anion and cation layers; two kinds of anions (A and B) form a zigzag-ABA′B′-array with dihedral angle (θ) of 42.6(1)° between the adjacent anions (A and B) along the *a*-axis. (c) Anion layer in **1**. Intermolecular contacts (Å): i, S7···Se7, 3.723(6); ii, S5···Se8, 3.795(5); iii, Se4···S13, 3.638(6); iv, S8···S11, 3.643(7); v, S2···Se6, 3.693(6); and vi, Se2···S10, 3.689(6). The Ni···Ni distances (Å) are a, 14.436; b, 12.562; c, 9.747; and d, 9.813. Reprinted with permission from Ref. [34] Copyright 2007 American Chemical Society.

ing state as a result of localization, one per [Ni(dmstfdt)$_2$] molecule, of the conduction electrons and further exhibits long-range magnetic ordering with a Néel ground state below 20 K.

2.4. Conducting dithiolenes containing a thiophenic moiety

Novel extended dithiolene ligands incorporating not only a TTF [35a] but also thiophenic moieties were also investigated since the evidence, observed by Almeida and coworkers, of the metallic state in [Au(α-tpdt)$_2$]$^\bullet$ (**12**) (α-tpdt = 3,4-thiophenedithiolate) [35b,c] a member of a novel class of gold complexes with thiophenedithiolate ligands, where the peripheral thiophene sulfur atoms promote additional intermolecular S···S contacts that controls the packing pattern and thus the electronic properties.[4] The extra thiophenic units were expected to enhance the degree of π-delocalization over the ligand extremity, while the presence of the additional thiophenic sulfur atom can favour the side intermolecular interactions at the ligand periphery, as found in other thiophene-type ligands based compounds [35–36]. The gold and nickel bisdithiolene complexes of the new highly extended ligands, α-tdt (2,3-thiophenetetrathiafulvalenedithiolate) and dtdt (dihydro-thiophenetetrathiafulvalenedithiolate) were synthesized by Almeida and coworkers and fully characterized. These complexes, were obtained under anaerobic conditions as monoanionic [^{n}Bu$_4$N][Au(α-tdt)$_2$] (**13a**), [^{n}Bu$_4$N][Au(dtdt)$_2$] (**14a**) and dianionic species [^{n}Bu$_4$N]$_2$[Ni(α-tdt)$_2$] (**13b**), [^{n}Bu$_4$N]$_2$[Ni(dtdt)$_2$] (**14b**) and subsequently oxidized to the stable neutral state by air or iodine exposure (Scheme 3). The monoanionic complexes crystallize in at least two polymorphs, showing a similar packing motif with a strong segregation of anions and cations in alternating layers which are connected through several hydrogen bonds. The anionic layers are composed of tightly packed parallel chains of the Nickel or Gold complexes which are almost parallel to the chain axis and form domino like-chains through an overlapping of their terminal thiophenic rings. In the case of **14b** the overlapping between anions occurs through both the thiophenic ring and part of the TTF moiety, with all of the sulfur atoms connected by S···S short contacts. Several side-by-side short S···S contacts are observed between parallel chains which give rise to extended 2D networks of contacts.

All of the neutral complexes, obtained by means of iodine oxidation, show room-temperature electrical conductivity of the order of 2, 2.5, 5 and 8 S cm^{-1} for [Ni(α-tdt)$_2$], [Ni(dtdt)$_2$], [Au(α-tdt)$_2$] and [Au(dtdt)$_2$], respectively. The more crystalline Ni samples, obtained by slow oxidation by air exposure, show higher electrical conductivity values of 200 S cm^{-1} for [Ni(dtdt)$_2$] with a clear

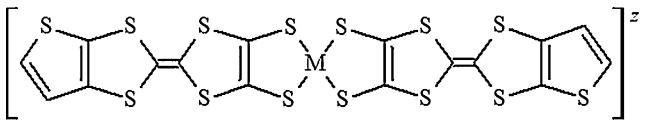

(12) [M(α-tdt)$_2$]^z, M= Au (**a**), Ni (**b**)

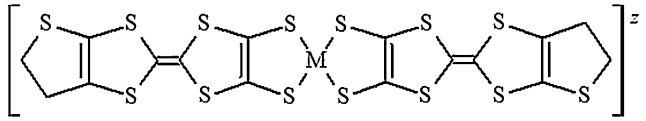

(13) [M(dtdt)$_2$]^z, M= Au (**a**), Ni (**b**)

Scheme 3.

[4] The conductivity measurements, performed on a polycrystalline sample, show that [Au(α-tpdt)$_2$]$^\bullet$ is a metal in the 15–300 K range with high room temperature conductivity, σ_{rt} = 6 S cm^{-1}, exceptionally large considering powder data are typically 100- to 1000-fold weaker than those observed in single crystals along their most conductive axis. This compound shows paramagnetic behaviour almost independent of the temperature down to 10 K, reminiscent of the Pauli paramagnetism typical of metallic systems. Unfortunately no crystal data were available to further investigate the origin of the metallic state [35].

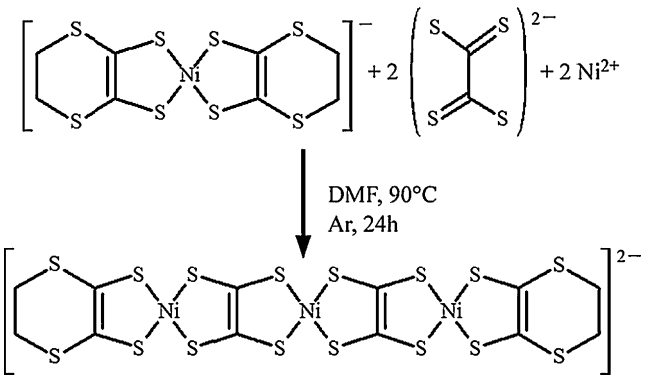

Scheme 4.

metallic behaviour down to 80 K and 24 S cm^{-1} for [Ni(α-tdt)$_2$], respectively. These complexes show also relatively large magnetic susceptibility values that correspond, beside the Pauli contribution of 2–5 × 10^{-4} emu mol^{-1}, typical of conducting systems, to effective magnetic moments in the range 1–3 μ_B, indicating that, in addition to delocalized conduction electrons, there are unpaired localized electrons. These compounds are new examples of single-component molecular metals where a 2D network of intermolecular interactions is related to high electrical conductivity. Other peculiar examples of these SCMMs are found in Ref. [37a,b].

2.5. Conducting multimetallic dithiolenes

Multimetallic complexes with extended π-conjugated dithiolene systems represent a new class of highly conducting single-component molecular materials whose large/long size provide multidimensional intermolecular interactions, new types of crystal structures and thus interesting electronic and/or magnetic properties. Kato and coworkers [38] have prepared and fully characterized novel trimetallic Ni^{II} complexes by reacting the corresponding monometallic Ni–dithiolene complex [Ni(S–S)$_2$]$^{n-}$ (n = 0 or 1, S–S = edo^2, dddt^{2-}) (edo^{2-} = 5,6-dihydro-1,4-dioxine-2,3-dithiolate) with the tetrathiooxalato (tto) ligand and a Ni^{II} cation (Scheme 4).

This reaction unexpectedly produced trinuclear complexes with two tto bridging ligands along with the binuclear complex. Structural results show that the anion of (Ph$_4$P)$_2$[Ni$_3$(tto)$_2$(dddt)$_2$] (**15**) is almost planar and the coordination around Ni(1) and Ni(2) is square-planar as expected for d^8 complexes. Theoretical calculations (*ab initio* and extended Hückel) show that this complex has a small HOMO–LUMO gap (0.15 eV) and highly symmetric HOMO and LUMO which are similar to those of [Ni(timdt)$_2$] (HOMO–LUMO gap = 0.10 eV), with a 3D π band. This is reflected by the conducting properties of this salt, a semiconductor with very high room-temperature conductivity (σ_{rt} = 1.0 × 10^4 S cm^{-1}) and very low activation energy (E_a = 0.28 eV). These trinuclear complexes with such an extended π-conjugated system represent a new class of highly conducting single-component molecular materials out of the mononuclear highly delocalized open-shell dithiolene complexes and metal–dithiolenes with extended-TTF donors, whose selected examples have been described at the beginning of this section.

3. H-bonding

In Sections 2.2 and 2.4 selected examples of compounds where H-bonding plays a role in determining 2D or 3D supramolecular architectures are reported. A magnetic exchange pathway through hydrogen bonds might be also responsible for the occurrence of magnetic ordering, as it has been observed in several compounds [39a–c]. Among them it is noteworthy the novel dithiolene complex with the organometallic bis(benzene)chromium(+) cation, bis(4,5-dimethoxybenzene-1,2-dithiolate) nickel(−), [Cr(η^6-C$_6$H$_6$)$_2$][Ni(dmox)$_2$] [40] (**16**) which represents, to the best of our knowledge, the first example of a metal bis(arene) complex showing ferromagnetically ordering (Scheme 5). It must be pointed out that magnetic ordering in organometallic compounds [41] is quite rare and the studies on the corresponding [Cr(η^6-C$_6$H$_6$)$_2$](TCNQ) system show an ordinary paramagnetic behaviour [42]. In [Cr(η^6-C$_6$H$_6$)$_2$][Ni(dmox)$_2$], the Ni–S bond distances, which fall in the 2.13–2.16 Å range typical for monoanionic systems, are in agreement with the 1-charge ascribed to the dmox complex [43]. The crystal structure consists of interpenetrating sublattices of anions and cations, each one well separated from the other of opposite charge, where the symmetry planes defined by the cations and anions are almost perpendicular to each other. In decamethyl metallocenium/dithiolene systems these planes are almost parallel, a common structural feature of compounds showing magnetic ordering [5]. H-bonding is crucial in determining the packing motif. There are three shortest contacts in the structure, each one involving a hydrogen atom of one of the aromatic rings of the cations and the heteroatoms (O, S, and Ni) of the dithiolene anions, leading to chain formation and thus to a 3D network. At T > 10 K [Cr(η^6-C$_6$H$_6$)$_2$][Ni(dmox)$_2$] (**16**) behaves as a paramagnet following the Curie–Weiss law for S = 1/2 on each ion (T_{Weiss} = 8.5 K) while magnetic susceptibility and magnetization studies evidentiate a transition to a ferromagnetically ordered phase at T = 3.4 K. It has been suggested that the structural motif of hydrogen bonds, especially the short contacts between anion heteroatoms (O and Ni) and cation H atoms (O–H = 2.437 Å; Ni–H = 2.908 Å) and the longer interionic S–H (3.148 and 3.260 Å) contacts, are responsible for the ferromagnetic interaction by mediating the magnetic communications between cations and anions.

The relevance of H-bonding in determining the magnetic properties of nitrile containing paramagnetic metal dithiolenes, as well as the capabilities of these complexes to work as ligands has been investigated by Fourmigué and coworkers. [Ni(mnt)$_2$]$^-$ has been successfully used to coordinate through the outer CN groups the metal in [Mn(III)(tpp)] (tpp = *meso*-tetraphenylporphinato) forming [Mn(III)(tpp)][Ni(mnt)$_2$]$_2$ (**17**) 1D polymer chains, which exhibit antiferromagnetic interaction and order as ferrimagnets at very low temperature (2–8 K) [44]. The solid state organization of [Ni(mnt)$_2$]$^-$ and ammonium or pyridinium cations has been also pointed out. In the [pyH$^+$][Ni(mnt)$_2$] (pyH$^+$ = pyridinium) compound (**18**) bifurcated NH···NC and C4H···NC hydrogen bonds are formed favouring the dimerization of the two radical complexes (Fig. 8), which show magnetic susceptibility in agreement with a singlet–triplet thermally activated behaviour [45]. The use of less conventional asymmetrical ligands containing two different groups attached at the same C$_2$S$_2$ moiety, such as the [Ni(edtCN)$_2$]$^{\bullet-}$ complex with only two nitrile substituents, when faced with one single hydrogen bond donor, still leads in both [HNMe$_3$][Ni(edtCN)$_2$]

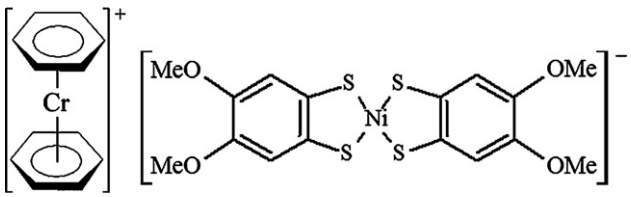

(16) [Cr(η^6-C$_6$H$_6$)$_2$][Ni(dmox)$_2$]

Scheme 5.

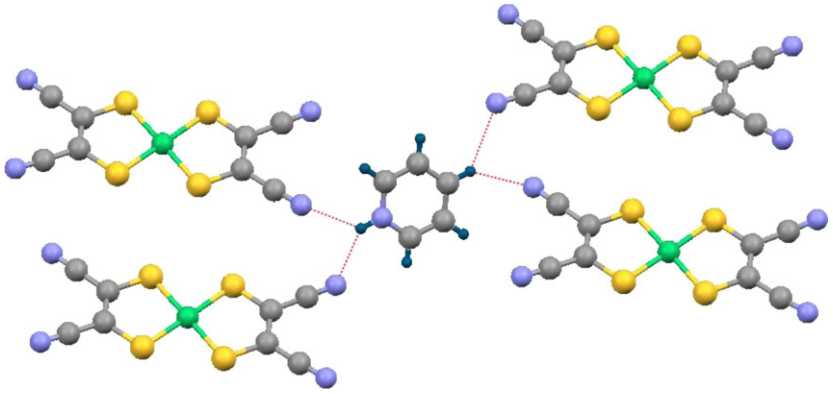

Fig. 8. Details of hydrogen bonds network in [pyH$^+$][Ni(mnt)$_2$] (**18**) (pyH$^+$ = pyridinium). Adapted with permission from Ref. [45]. Copyright 2003 American Chemical Society.

and [PyH][Ni(edtCN)$_2$] salts to bifurcated NH···NC hydrogen bonds which control the structural organization. The structural requirements imposed by these hydrogen bond motifs reflect in the magnetic properties of the salts, leading either to noninteracting or to strongly dimerized, singlet–triplet activated systems.

4. π–d Interactions

The development of π–d systems as multifunctional materials represents one of the main targets in current materials science for their potential applications for future molecular electronics. The most common approach, the molecular approach, used for obtaining such materials, consists in combining two molecular networks, each one furnishing a distinct physical property to the resulting materials. The first paramagnetic superconductor (ET)$_4$[H_3OFe^{III}(C_2O_4)$_3$]·C_6H_5CN [12a] and the first ferromagnetic conductor (BEDT-TTF)$_3$[CrMn(C_2O_4)$_3$] [14] were successfully obtained by combining the mononuclear [Fe(C_2O_4)$_3$]$^{3-}$ chiral anion and the 2D honeycomb anion with oxalate bridges [Cr^{III}Mn^{II}(C_2O_4)$_3$]$_n$, respectively as the magnetic building blocks with the BEDT-TTF molecule as the conducting building block. Furthermore, by using the BEDT-TSF molecule with the zero-dimensional $FeCl_4^-$ anion, a field-induced superconductivity with π–d interaction was observed which may be mediated through S···Cl interactions between the BEDT-TSF molecule and the anion [46]. Selected examples of multifunctional materials where the π-electron interaction with localized 3d moments is caused by close contact between chalcogen atoms and magnetic anions will be discussed in this section. Dual-function materials were recently obtained by B. Zhang and coworkers [47] by combining TTF and BETS molecules with the 1D [Fe^{III}-(C_2O_4)Cl_2^-]$_n$ magnetic chain anions, containing both the oxalate ligand and the Cl^- anion with the aim to introduce the magnetic interaction by the oxalate bridges between moment-carriers as well as the π–d interaction through S···Cl contacts. When using the BETS molecule, the first weak-ferromagnetic organic conductor κ-(BETS)$_2$[Fe^{III}-(C_2O_4)Cl_2] (**19**) was obtained. The structure consists of BETS molecules stacks, arranged in a 2D κ-phase, slightly different from that of the κ-(BETS)$_2$[$FeBr_4$] [13]; there are Se···Se contacts within the BETS dimers and Se···S, S···S between dimers in one layer where the 1D [Fe^{III}-(C_2O_4)Cl_2^-]$_n$ chain anions fits in the channel between the two BETS layers (Fig. 9). κ-(BETS)$_2$[Fe^{III}-(C_2O_4)Cl_2] is a molecular conductor with $\sigma_{300K} = 10^2$ S cm^{-1} and it retains the metallic state down to 2 K, in good agreement with the calculated band structures [48]. The susceptibility data in the 400–25 K range were fitted to a model of a 1D antiferromagnetic $S = 5/2$ chain plus a contribution from a Curie impurity as well as a temperature-independent term. The long-range magnetic ordering below 5 K can only be ascribed to the presence of π–d interaction through S···Cl interaction between BETS molecules and anions, because, theoretically, no long-range order is possible at any temperature for a 1D-magnetic system. κ-(BETS)$_2$[Fe^{III}-(C_2O_4)Cl_2] is the first organic conductor showing weak-ferromagnetism deriving from the two-sublattices.

Coexistence of conducting π-electrons and localized 3d moments has been found in the novel α-(BEDT-TTF)$_5$[Fe(C_5O_5)$_3$]·5H_2O (**20a**) and β-(BEDT-TTF)$_5$[Fe(C_5O_5)$_3$]·C_6H_5CN (**20b**) [49] dual-function materials containing the new paramagnetic and chiral anion [Fe(C_5O_5)$_3$]$^{3-}$ ($C_5O_5^{2-}$ = croconate). This anion contains the croconate ligand whose coordination modes and ability to mediate magnetic interactions [50] are very similar to the oxalate one. The structure of both compounds consists of alternating layers of BEDT-TTF molecules separated by layers of [Fe(C_5O_5)$_3$]$^{3-}$ anions and solvent (water for **37a**, C_6H_5CN for **37b**) molecules where a shortest interanion O···O distance (O4–O5) of 3.122 Å is found. The BEDT-TTF molecules in **1** are arranged in a herring-bone packing motif, typical of the α-phase, which is induced by the chirality of the anions. The [Fe(C_5O_5)$_3$]$^{3-}$ anions form zigzag rows, separated by water molecules, along the c direction with Δ enantiomers alternating with the Λ ones, giving rise to an achiral structure. Thus, each Δ enantiomer induces a "right-turned" column of BEDT-TTF molecules in the organic layer above and a "left-turned" column in the layer below. Of course, the Λ enantiomer induces the opposite packing scheme. This effect is possible thanks to the presence of a supramolecular interlayer S···O cation–anion interaction

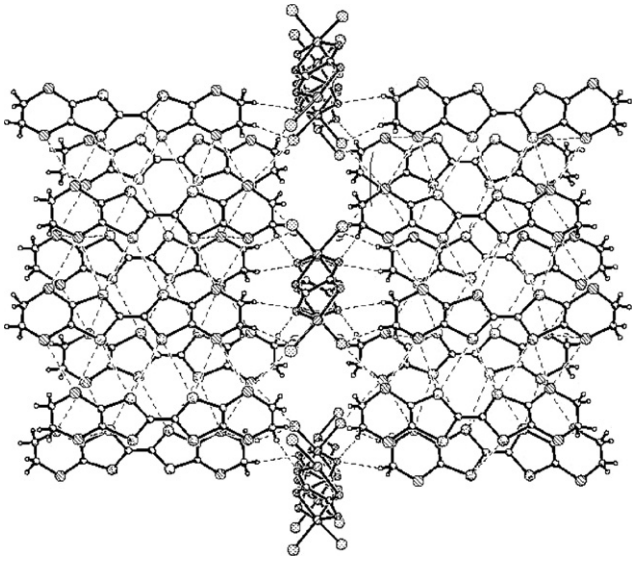

Fig. 9. View of the packing of κ-(BETS)$_2$[Fe^{III}-(C_2O_4)Cl_2] (**19**) along the *c*-axis. Reprinted with permission from Ref. [47]. Copyright 2007 Elsevier.

(S15–O5 = 3.01 Å), much shorter than the sum of the corresponding van der Waals radii (3.32 Å) together with the steric effects. Therefore, the alternation of Δ and Λ enantiomers along the *b*-axis is the driving force that induces the same alternation of "right" and "left" turned columns along this direction, giving rise to the α-packing observed in the organic sublattice in **20a** as shown in Fig. 10. As far as we know **20a** represents the first example of chirality-induced α-phase and the only known pentamerized (θ_{51}) phase. No influence of the chirality of the anions instead has been found in **20b**.

Several intermolecular interactions are found in **20b** between the organic, inorganic layers and solvent molecules. Besides the S···N contact (S57–N8 = 3.21(2) Å) between one BEDT-TTF molecule (ET5) and the N atom of the C_6H_5CN solvent molecule, there are up to five S···O cation–anion interactions in the range 2.887–3.208 Å, shorter than the sum of the van der Waals radii (3.32 Å). Although the room-temperature conductivity of **20a** (ca. 6 S cm^{-1}) is quite high, the thermal variation of the resistivity shows a continuous decrease with decreasing the temperature and shows a classical semiconducting regime with an activation energy of 116 meV. The thermal variation of the resistivity, reported in Fig. 11, shows that **20b** is metallic down to ca. 120 K. Below this temperature the conductivity becomes thermally activated although it does not follow an Arrhenius law ($\ln\sigma \propto T^{-1}$) nor a hopping regime where $\ln\sigma \propto T^{-\alpha}$ (with $\alpha = 1/3$ or 1/4). Furthermore, the reentrance to the metallic state observed below ca. 20 K supports the idea that the minimum in the resistivity at ca. 120 K is not a true metal-semiconductor transition as supported by the current dependence of this reentrance.

This kind of behaviour, although unusual, has already been observed in other related BEDT-TTF salts with the chiral anions $[M(C_2O_4)_3]^{3-}$ (M^{III} = Ga, Fe, and Cr) [12,18]. The susceptibility data indicates that **20a** and **20b** are $S = 5/2$ paramagnets but **20b** shows an extra temperature-independent paramagnetic contribution (Pauli-type paramagnetism) typical of metallic salts. **20b** is one of the very few examples of paramagnetic molecular metals and the only known example out of the $[M(C_2O_4)_3]^{3-}$ and $[MX_4]^{n-}$ series.

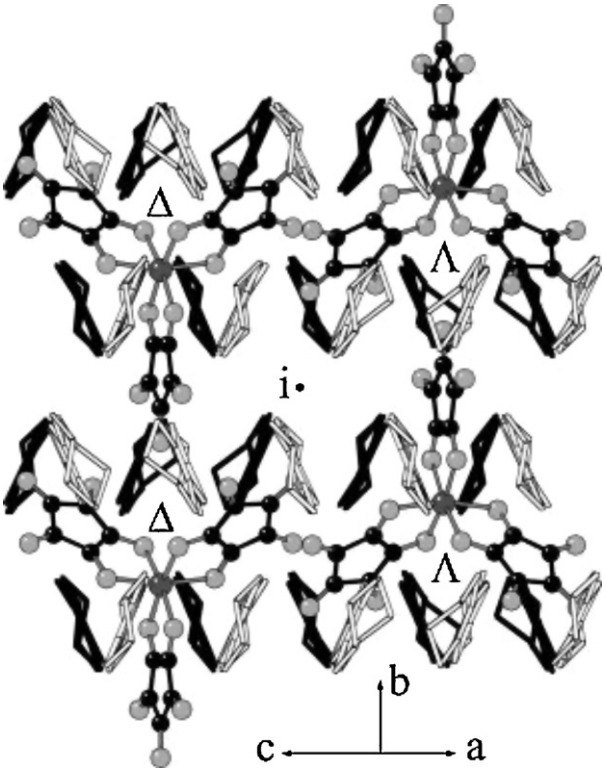

Fig. 10. View of the anionic layer of **20a** showing the zigzag rows of anions with alternating chirality and the organic layers above (white) and below (black) the anionic layer. The point indicates the location of the inversion center in the anionic layer. Reprinted with permission from Ref. [49]. Copyright 2007 American Chemical Society.

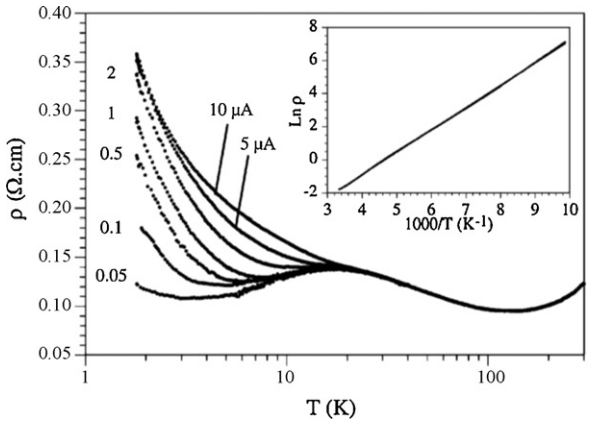

Fig. 11. Thermal variation of the dc resistivity at different current intensities (in μA) for **20b**. Inset: Arrhenius plot of the thermal variation of the resistivity of **20a**. Reprinted with permission from Ref. [49]. Copyright 2007 American Chemical Society.

Coexistence of delocalized and localized unpaired d electrons has been found in the $(TTF)_2[Fe(tdas)_2]$ (**21**) (tdas is 1,2,5-thiadiazole-3,4-dithiolate) [51] compound containing the peculiar $[Fe(tdas)_2]^-$ dithiolene anion which exhibits unusual magnetic properties. Its tetrabutylammonium TBA$[Fe(tdas)_2]$ salt (**22**) [52], which exhibits a dimeric structure and magnetic properties typical of an antiferromagnetic dimer, shows two unusual phase transitions in the 190–240 K range. These transitions have been explained as a reentrant phase behaviour, where the low- and high-temperature phase are identical while a second phase with a different value of the antiferromagnetic exchange coupling constant exists at intermediate temperatures. Structural data and magnetic measurements show that this compound consist of antiferromagnetic $[Fe(tdas)_2]_2^{2-}$ dimers separated by organic TTF layers and behaves as a semiconductor. An increase in the number of S atoms in the TTF molecule should increase the intermolecular interactions leading to metal-like behaviour. Thus when the BEDT-TTF molecule, which contains eight sulfur atoms (twice the number of TTF) and an extended π-system, is used, the obtained $(BEDT\text{-}TTF)_2[Fe(tdas)_2]$[5] (**23**) [53] still shows semiconducting behaviour over the whole temperature range, but the extended sulfur framework of BEDT-TTF, as compared to TTF, allows for increased side-to-side sulfur–sulfur interactions leading to improved electrical conductivity: room-temperature conductivity for the BEDT-TTF salt is about 1 S cm^{-1} as compared to 0.03 S cm^{-1} for the TTF analogue. Substitution of the S atoms by Se is expected to result in increased polarizabilities and orbital overlap between molecules, leading to stable metallic states. Thus, by using BETS, where four of the eight atoms of ET are replaced by Se, metal-like behaviour should be achieved. $(BETS)_2[Fe(tdas)_2]_2$ (**24**) [54], which consists of segregated columns of dimers of BETS and columns of dimers of $[Fe(tdas)_2]$, shows metal-like behaviour. Numerous chalcogen–chalcogen contacts are observed within and between the columns, responsible for the high room-temperature conductivity (0.2 S cm^{-1}) and the metallic character which is observed down to ca 200 K. The relationship between interaction modes and physical properties of (BEDT-TTF)$[Ni(tdas)_2]$ (**4**) compound has

[5] $(BEDT\text{-}TTF)_2[Fe(tdas)_2]$ consists of conducting, organic BEDT-TTF layers separated by dimerized, magnetic $[Fe(tdas)_2]_2^{2-}$ anions.

Table 1
Interaction modes and physical properties of chalcogenolene-based molecular materials.

Compound	Interaction modes (packing)	Physical properties	Reference
Cs^{+}_2(B[18]crown-6)$_3$[Ni(dmit)$_2$] (**1**)	Lateral S···S contacts (2D arrangement) π-dimer chain (1D network)	FM coupling (T = +1.1 K) AFM coupling (J = −5.2 K)	[20]
Cs^{+}_2(DB[18]crown-6)$_3$[Ni(dmit)$_2$] (**2**)	Lateral S···S contacts (1D dimer chain)	AFM coupling (J = −25.5 K) (dimer model)	[20]
(Ph-NH_3)$^{+}$(DCH[18]-crown-6)[Ni(dmit)$_2$] (**3**)	Lateral S···S contacts along the short axis	FM coupling (T = +0.9 K)	[21]
(BEDT-TTF)[Ni(tdas)$_2$] (**4**)	Isolated monoanions	–	[22]
	Lateral S···N contacts (Layered structure, 1D network)	AFM coupling (dimer model) Semiconductor (σ_{RT} = 0.018 S cm^{-1}), semiconductor–semiconductor transition (200 K)	
(HBzPy)[Ni(α-tpdt)$_2$] (**5a**)	π–π interactions, S···H–C hydrogen bonds	FM coupling	[24]
(BrBzPy)[Ni(α-tpdt)$_2$] (**5b**)	π–π interactions, C–Br···S contacts	AFM coupling (anomaly at 6 K)	
(FBzPy)[Ni(α-tpdt)$_2$] (**5c**)	π–π interactions, C–Br···S contacts (alternated layers of anions and cations)	PM down to 1.5 K	
[Ni(tmdt)$_2$] (**7a**)	π–π interactions, S···S contacts (3D network)	PM metallic down to 0.6 K (σ_{RT} = 400 S cm^{-1})	[26]
[Au(tmdt)$_2$] (**7b**)	π–π interactions, S···S contacts (3D network)	AFM phase transition at 110 K σ_{RT} = 200 S cm^{-1}	[28]
[Cu(dmdt)$_2$] (**8**)	π–π interactions, intra- and interlayer S···S contacts ("κ-type" arrangement)	Curie–Weiss PM (84% of S = 1/2 spin moments) Semiconductor (σ_{RT} = 3 S cm^{-1})	[27]
(^{n}Bu$_4$N)[Ni(chdt)$_2$] (**9b**)	Side-by-side S···S contacts along the *c*-axis and interchain (sandwiched structure)	AFM 1D Heisenberg chain	[32]
(^{n}Bu$_4$N)[Ni(eodt)$_2$] (**10b**)		Curie–Weiss PM	
(^{n}Bu$_4$N)[Ni(dmstfdt)$_2$] (**11**)	Intermolecular S···S(Se) contacts (2D layered structure)	PM (Curie-Weiss), weak FM coupling (T_N = 20 K) weak metal behaviour down to 147 K	[34]
(Ph$_4$P)$_2$[Ni$_3$(tto)$_2$(dddt)$_2$] (**15**)	Extended π-conjugated system (layered structure)	Semiconductor (σ_{RT} = 1.0 × 10^4 S cm^{-1})	[38]
[Cr(η^6-C$_6$H$_6$)$_2$][Ni(dmox)$_2$] (**16**)	Cation–anion hydrogen bonds (H···O, H···S, H···Ni) (3D network formed by chains)	PM (Curie–Weiss) for 1D chains at T > 10 K; FM transition at T = 3.4 K	[40]
[Mn(III)(tpp)][Ni(mnt)$_2$]$_2$ (**17**)	Metal coordination through CN (1D polymer chains)	AFM, FM ordering at 2–8 K	[44]
[pyH^{+}][Ni(mnt)$_2$] (**18**)	Bifurcated NH···NC and C4H···NC hydrogen bonds	Singlet–triplet thermally activated behaviour	[45]
κ-BETS$_2$[Fe^{III}-(C$_2$O$_4$)Cl$_2$] (**19**)	π–d interactions through S···Cl contacts between BETS and anions	Weakly FM	[47,48]
	Se···Se contacts, Se···S, S···S contact (2D κ-phase of BETS)	Metal (σ_{300K} = 10^2 S cm^{-1}), retains the metallic state down to 2 K	
α-(BEDT-TTF)$_5$[Fe(C$_5$O$_5$)$_3$]·5H$_2$O (**20a**)	Interlayer S···O cation–anion interaction (herring-bone packing motif, α-phase)	PM σ_{RT} = 6 S cm^{-1}	[49]
β-(BEDT-TTF)$_5$[Fe(C$_5$O$_5$)$_3$]·C$_6$H$_5$CN (**20b**)	S···N contacts BEDT-TTF-solvent, S···O cation–anion interactions (β-phase)	PM metal down to 120 K	
(BEDT-TTF)$_2$[Fe(tdas)$_2$] (**23**)	Side-by-side S···S interactions	σ_{RT} = 1 S cm^{-1}	[53]
(BETS)$_2$[Fe(tdas)$_2$]$_2$ (**24**)	Se···Se, Se···S, S···S contacts (segregated columns of cations and anions)	σ_{RT} = 0.2 S cm^{-1}, retains the metallic state down to 200 K	[54]
(Me-3,5-DIP)[Ni(dmit)$_2$]$_2$ (**23**)	Supramolecular halogen I···S interactions	PM with AFM interactions 2D metallic conductivity	[55]
{[Mn$_4$]$^{4+}$} {Pt(mnt)$_2$}$_4$][Pt(mnt)$_2$]$_2$ (**24**)	Interaction *via* conducting electrons (1D stacks of anions along the *a*-axis)	SMM character of the [Mn$_4$]$^{4+}$ unit Semiconductor down to 110 K (insulator at T < 110 K), σ_{RT} = 0.2 S cm^{-1}	[56]

PM, paramagnetic; FM, ferromagnetic; AFM, antiferromagnetic.

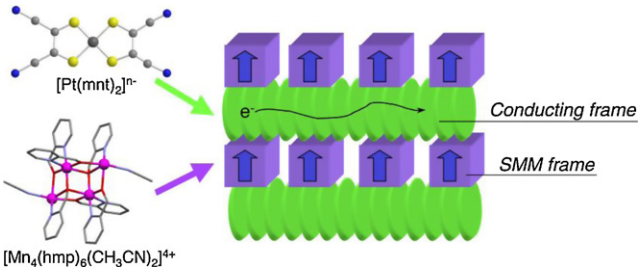

Scheme 6. Reprinted with permission from Ref. [56]. Copyright 2007 American Chemical Society.

been already discussed in Section 2.1 [22]. It is noteworthy how the charge-compensating molecular cation controls the network formation and determines the conducting properties of the resulting molecular material. When using *N*-methyl-3,5-diiodopyridinium (Me-3,5-DIP), the introduction of supramolecular halogen I···S interactions into the Ni(dmit)$_2$ complex has yielded a peculiar magnetic molecular conductor (Me-3,5-DIP)[Ni(dmit)$_2$]$_2$ (**25**) [55], without localized d moments. Two kinds of layers of Ni(dmit)$_2$ anions are present in this salt. Two-dimensional metallic conductivity and paramagnetism with antiferromagnetic interactions both are derived solely from molecular π-electrons of Ni(dmit)$_2$ anions contained separately in each layer. This is the first system where conducting and magnetic π-electrons coexist down to 4.2 K.

Yamashita and coworkers have reported on the synthesis of a unique hybrid material based on Mn_4 single-molecule magnet (SMM) clusters having $S_T = 9$ spin state and [Pt(mnt)$_2$]$^{n-}$ dithiolene complexes, [{($Mn^{II}_2Mn^{III}_2$(hmp)$_6$(MeCN)$_2$} {Pt(mnt)$_2$}$_4$][Pt(mnt)$_2$]$_2$ (**26**), (hmp$^-$ = 2-hydroxymethyl pyridinate) [56] showing SMM/semiconducting behaviour (Scheme 6).

Recent studies have demonstrated that the inter-SMM interaction *via* conducting electrons, albeit small, has a mutual influence on both SMM properties and conductivity [57a,b]. The structure consists of [$Mn^{II}_2Mn^{III}_2$(hmp)$_6$(MeCN)$_2$]$^{4+}$ ([Mn_4]$^{4+}$) units separated by 1D double columns of [Pt(mnt)$_2$]$^{n-}$ complexes. There are two [Pt(mnt)$_2$]$^{n-}$ units (**A** and **B**) coordinated with the Mn^{II} ion of the [Mn_4]$^{4+}$ unit forming a discrete unit, {[Pt(mnt)$_2$]$_2$-[Mn_4]-[Pt(mnt)$_2$]$_2$}. The uncoordinated [Pt(mnt)$_2$]$^{n-}$ (**C**) and coordinated **A** and **B** are mutually stacked along the *a*-axis (Fig. 12a) to form a segregated one-dimensional double column possessing an [···**A**···**B**···**C**···] repeating unit (Fig. 12b). Considering the charge balance and the structures of **A**, **B**, and **C**, the [Pt(mnt)$_2$] units show a fractional charge of −0.66. The electron transport properties of this salt, measured along the [Pt(mnt)$_2$]$^{0.66-}$ columns (stacking *a*-axis), show that it is a semiconductor down to 110 K (insulator at $T < 110$ K) with high room-temperature conductivity ($\sigma_{rt} = 0.2$ S cm^{-1}) and activation energy $E_a = 136$ meV. The temperature dependence of χT shows a typical intra-cluster ferromagnetic behaviour, already seen in related [Mn_4] clusters [58]. Examination of the magnetic behaviour at low temperatures show the SMM character of the [Mn_4]$^{4+}$ unit and possible inter-unit interactions. Partially oxidized [Pt(mnt)$_2$]$^{n-}$ subunits allowing conductivity are rare and only Li salts of [Pt(mnt)$_2$]$^{n-}$ have been reported so far [59]. However, the conductivity was present only in the temperature region where the SMM unit behaved as a general paramagnet. In addition, both components of SMM and conducting network acted independently in the entire temperature range.[6]

[6] Single-molecule magnets (SMMs) [60a] and single-chain magnets (SCMs) [60b] are challenging research targets because of their potential applications as ultimate memory devices or in quantum computation due to their intrinsic large spin state and uni-axial anisotropy.

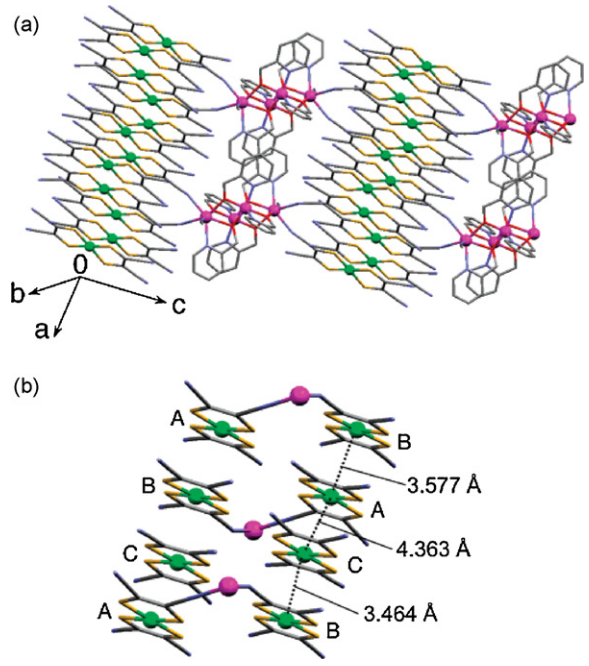

Fig. 12. Packing view of [{($Mn^{II}_2Mn^{III}_2$(hmp)$_6$(MeCN)$_2$}{Pt(mnt)$_2$}$_4$][Pt(mnt)$_2$]$_2$ (**26**), (a) and arrangement of part of [Pt(mnt)$_2$]$^{n-}$ moieties (b). Reprinted with permission from Ref. [56]. Copyright 2007 American Chemical Society.

The preparation of this compound is very challenging and opens the doors to the design of superparamagnetic/highly conductive hybrid materials.

The interaction modes, the packing pattern and physical properties of the compounds discussed in this work are summarized in Table 1.

5. Concluding remarks

The compounds described in this work, summarized in Table 1, clearly show that the biggest challenge of molecule-based materials can be envisaged in the design and synthesis of the molecular building blocks. Molecules with the desired size, shape, charge and electronic properties determine the intermolecular interactions and the strength and directionality of these interactions yield to the supramolecular structure of the material, targeting for its desired properties. The intermolecular interactions, therefore, in particular van der Waals interactions, π–π and π–d interactions, H-bonding, *etc.*, play a crucial role in self-assembling these pre-designed molecular units and may provide a powerful way to afford layered molecular materials with new or unknown physical properties. The examples reported in Table 1 show that in those compounds where S···S and π–π stacking interactions occur between the two anionic and cationic networks, transitions to long-range magnetic order are observed. In the case of H-bonding it was suggested that 2D or 3D structural motifs of hydrogen bonds, especially short contacts between anion heteroatoms and cation H atoms are responsible for the occurrence of magnetic order by mediating the magnetic communications between cations and anions. The intermolecular chalcogen–chalcogen S(O)···S(O, Se) interactions in addition to other contacts such as S···I, S···O, S···N,··· between adjacent molecules which yielded to 2D or 3D networks, are also responsible for the occurrence of the metallic state up to low temperatures observed in single-component molecular metals and molecular magnetic conductors.

Future work must take the opportunity to build on the current understanding of the way these molecules assemble. Thus new

studies must be increasingly target driven and involve preparation of particular material types by rational analysis of the known behaviour of the component building blocks or by synthesis of new building blocks expected to interact in the solid state through the above-mentioned intermolecular interactions in a predetermined way. However BEDT-TTT, BETS, dithiolene complexes and polymeric metal oxalate complexes still remain the most successful molecular bricks to play with since their assemblage through the above-mentioned intermolecular interactions, might yield materials with exotic properties out of SCMM, long-range magnetic ordering materials and magnetic molecular conductors which are of utmost importance for the development of applications in molecular electronics, spintronics and other related areas of current interest in material science.

Acknowledgements

This work was supported by the University of Cagliari, MIUR (PRIN-2005033820_002 "Molecular materials with magnetic, optical and electrical properties"), Fondazione Banco di Sardegna and the COST Action D35, WG11 "Multifunctional and Switchable Molecular Materials". Thanks are specially due to the Guest Editor, Antonin Vlcék for its kind invitation to give a contribution to this Coordination Chemistry Reviews, Special Issue "Dithiolenes and non-innocent redox-active ligands".

References

[1] J.P. Ferraris, D.O. Cowan, V. Walatka Jr., J.H. Perlstein, J. Am. Chem. Soc. 95 (1973) 948.
[2] D. Jérome, M. Mazaud, M. Ribault, K. Bechgaard, J. Phys. Lett. 41 (1980) L95.
[3] L. Brossard, M. Ribault, M. Bousseau, L. Valade, P. Cassoux, C.R. Acad. Sci., Ser. II 302 (1986) 205.
[4] H. Tajima, M. Inokuchi, A. Kobayashi, T. Ohta, R. Kato, H. Kobayashi, H. Kuroda, Chem. Lett. (1993) 1235.
[5] C. Faulmann, Z.P. Cassoux, in: E.I. Stiefel (Ed.), Dithiolene Chemistry: Synthesis, Properties and Applications, Progress in Inorganic Chemistry, vol. 52, Wiley, Chichester, 2004, pp. 399–489.
[6] A.T. Coomber, D. Beljonne, R.H. Friend, J.L. Brédas, A. Charlton, N. Robertson, A.E. Underhill, M. Kurmoo, P. Day, Nature 380 (1996) 144.
[7] C. Faulmann, E. Rivière, S. Dorbes, F. Senoca, E. Coronado, P. Cassoux, Eur. J. Inorg. Chem. (2003) 2880.
[8] (a) M. Almeida, V. Gama, R.T. Henriques, L. Alcácer, in: R. Laine (Ed.), Inorganic and Organometallic Polymers with Special Properties, Kluwer Academic Publishers, Boston, 1992, p. 163;
(b) V. Gama, R.T. Henriques, G. Bonfait, L.C. Pereira, J.C. Waerenborgh, I.C. Santos, M.T. Duarte, J.M.P. Cabral, M. Almeida, Inorg. Chem. 31 (1993) 2598;
(c) V. Gama, R.T. Henriques, M. Almeida, L. Alcácer, J. Phys. Chem. 98 (1994) 997.
[9] R.E. Peierls, Quantum Theory of Solids, Oxford University Press, 1955, p. 108.
[10] (a) H. Kobayashi, H. Tomita, T. Naito, A. Kobayashi, F. Sakai, T. Watanabe, P. Cassoux, J. Am. Chem. Soc. 118 (1996) 368;
(b) T. Courcet, I. Malfant, K. Pokhodnia, P. Cassoux, New J. Chem. (1998) 585;
H. Fujiwara, E. Ojima, H. Kobayashi, T. Courcet, I. Malfant, P. Cassoux, Eur. J. Inorg. Chem. (1998) 1631.
[11] N.J. Harris, A.E. Underhill, J. Chem. Soc., Dalton Trans. (1987) 1683.
[12] (a) A.W. Graham, M. Kurmoo, P. Day, J. Chem. Soc., Chem. Commun. (1995) 2061;
(b) T. Enoki, A. Miyazaki, Chem. Rev. 104 (2004) 5449;
H. Kobayashi, H.B. Cui, A. Kobayashi, Chem. Rev. 104 (2004) 5265;
(c) M. Kurmoo, A.W. Graham, P. Day, S.J. Coles, M.B. Hursthouse, J.L. Caulfield, J. Singleton, F.L. Pratt, W. Hayes, L. Ducasse, P. Guionneau, J. Am. Chem. Soc. 117 (1995) 12209;
(d) L. Martin, S.S. Turner, P. Day, F.E. Mabbs, E.J.L. McInnes, J. Chem. Soc., Chem. Commun. (1997) 1367;
(e) S. Rashid, S.S. Turner, P. Day, J.A.K. Howard, P. Guionneau, E.J.L. McInnes, F.E. Mabbs, R.J.H. Clark, S. Firth, T. Biggs, J. Mater. Chem. 11 (2001) 2095.
[13] H. Fujiwara, E. Fujiwara, Y. Nakazawa, B.Zh. Narymbetov, K. Kato, H. Kobayashi, A. Kobayashi, M. Tokumoto, P. Cassoux, J. Am. Chem. Soc. 123 (2001) 306.
[14] E. Coronado, J.R. Galán-Mascarós, C.J. Gómez-García, V.N. Laukhin, Nature 408 (2000) 447.
[15] N. Robertson, L. Cronin, Coord. Chem. Rev. 227 (2002) 93.
[16] R. Kato, Chem. Rev. 104 (2004) 5319.
[17] A. Kobayashi, E. Fujiwara, H. Kobayashi, Chem. Rev. 104 (2004) 5243.
[18] E. Coronado, P. Day, Chem. Rev. 104 (2004) 5419.
[19] E. Coronado, J.-R. Galán-Mascarós, C.R. Chimie 11 (2008) 1110.
[20] T. Akutagawa, K. Shitagami, M. Aonuma, S. Noro, T. Nakamura, Inorg. Chem. 48 (2009) 4454.
[21] T. Akutagawa, D. Sato, H. Koshinaka, M. Aonuma, S. Noro, S. Takeda, T. Nakamura, Inorg. Chem. 47 (2008) 5951.
[22] M.L. Mercuri, P. Deplano, L. Pilia, A. Serpe, S. Curreli, J.A. Schlueter, M.A. Whited, U. Geiser, E. Coronado, C.J. Goméz-García, E. Canadell, Inorg. Chem. 43 (2004) 2049.
[23] Z. Ni, X.M. Ren, J. Ma, J. Xie, C. Ni, Z. Chen, Q. Meng, J. Am. Chem. Soc. 127 (2005) 14330.
[24] D. Belo, M.J. Figueira, J.P.M. Nunes, I.C. Santos, L.C. Pereira, M. Almeida, V. Gama, C. Rovira, J. Veciana, J. Mater. Chem. 16 (2006) 2746.
[25] A. Kobayashi, H. Tanaka, M. Kumasaki, M. Torii, B. Narymbetov, T. Adachi, J. Am. Chem. Soc. 121 (1999) 10763.
[26] H. Tanaka, Y. Okano, A. Kobayashi, W. Suzuki, H. Kobayashi, Science 291 (2001) 285.
[27] H. Tanaka, A. Kobayashi, H. Kobayashi, J. Am. Chem. Soc. 124 (2002) 10002.
[28] Y. Hara, K. Miyagawa, K. Kanoda, M. Shimamura, B. Zhou, A. Kobayashi, H. Kobayashi, J. Phys. Soc. Jpn. 77 (2008) 053706-1.
[29] B. Zhou, M. Shimamura, E. Fujiwara, A. Kobayashi, T. Higashi, E. Nishibori, M. Sakata, H. Cui, K. Takahashi, H. Kobayashi, J. Am. Chem. Soc. 128 (2006) 3872.
[30] S. Ishibashi, H. Tanaka, M. Kohyama, M. Tokumoto, A. Kobayashi, H. Kobayashi, K. Terakura, J. Phys. Soc. Jpn. 74 (2005) 843.
[31] K. Miyagawa, A. Kawamoto, Y. Nakazawa, K. Kanoda, Phys. Rev. Lett. 75 (1995) 1174.
[32] E. Fujiwara, A. Kobayashi, H. Fujiwara, H. Kobayashi, Inorg. Chem. 43 (2004) 1122.
[33] W.E. Estes, D.P. Gavel, W.E. Hatfield, D. Hodgson, Inorg. Chem. 17 (1978) 1415.
[34] E. Fujiwara, K. Yamamoto, M. Shimamura, B. Zhou, A. Kobayashi, K. Takahashi, Y. Okano, H. Cui, H. Kobayashi, Chem. Mater. 19 (2007) 553.
[35] (a) N. Le Narvor, N. Robertson, T. Weyland, J.D. Kilburn, A.E. Underhill, M. Webster, N. Svenstrup, J. Becher, J. Chem. Soc., Chem. Commun. (1996) 1363;
(b) D. Belo, H. Alves, E.B. Lopes, M.T. Duarte, V. Gama, R.T. Henriques, M. Almeida, A. Pérez-Benítez, C. Rovira, J. Veciana, Chem. Eur. J 7 (2001) 511;
(c) D. Belo, H. Alves, E.B. Lopes, M.T. Duarte, V. Gama, R.T. Henriques, M. Almeida, A. Pérez-Benítez, C. Rovira, J. Veciana, Synth. Met. 120 (2001) 699.
[36] D. Belo, M.J. Figueira, J. Mendonça, I.C. Santos, M. Almeida, R.T. Henriques, M.T. Duarte, C. Rovira, J. Veciana, Eur. J. Inorg. Chem. (2005) 3337.
[37] D. Belo, M.J. Figueira, J.P.M. Nunes, I.C. Santos, M. Almeida, N. Crivillers, C. Rovira, Inorg. Chim. Acta 360 (2007) 3909.
[38] K. Kubo, A. Nakao, H.M. Yamamoto, R. Kato, J. Am. Chem. Soc. 128 (2006) 12358.
[39] (a) T. Okamura, Y. Takano, Y. Yoshika, N. Ueyama, A. Nakamura, K. Yamaguchi, J. Organomet. Chem. 569 (1998) 177;
(b) M. Deumal, M.A. Robb, J.J. Novoa, Polyhedron 22 (2003) 1935, and references therein;
(c) J.F. Ferrer, P.M. Lahti, C. George, P. Oliete, M. Julier, F. Palacio, Chem. Mater. 13 (2001) 2447.
[40] N.C. Schiødt, R. Sessoli, F.C. Krebs, Inorg. Chem. 43 (2004) 1986.
[41] D. O'Hare, J.S. Miller, Mol. Cryst. Liq. Cryst. 176 (1989) 381.
[42] A.V. Zvarykina, Yu.S. Karimov, R.B. Ljubovsky, M.K. Makova, M.L. Khidekel, I.F. Shchegolev, E.B. Yagubsky, Mol. Cryst. Liq. Cryst. 11 (1970) 217.
[43] D. Sellmann, H. Binder, D. Haussinger, F.W. Heinemann, J. Sutter, Inorg. Chim. Acta 300 (2000) 829.
[44] L. Dawe, J. Miglioi, L. Turnbow, M.L. Taliaferro, W.W. Shum, J.D. Bagnato, L.N. Zakharov, A.L. Rheingold, A.M. Arif, M. Fourmigué, J.S. Miller, Inorg. Chem. 44 (2005) 7530.
[45] M. Fourmigué, C. Mézière, S. Dolou, Cryst. Growth Des. 3 (2003) 805.
[46] S. Uij, H. Shinagawa, T. Terashima, T. Yakabe, Y. Terai, M. Tokumoto, A. Kobayashi, H. Tanaka, H. Kobayashi, Nature 410 (2001) 908.
[47] B. Zhang, Z. Wang, Y. Zhang, H. Kobayashi, M. Kurmoo, T. Mori, F.L. Pratt, K.I.D. Zhu, Polyhedron 26 (2007) 1800.
[48] B. Zhang, Z.M. Wang, Y. Zhang, K. Takahashi, Y. Okano, H.B. Cui, H. Kobayashi, K. Inoue, M. Kurmoo, F.L. Pratt, D.B. Zhu, Inorg. Chem. 45 (2006) 3275.
[49] E. Coronado, S. Curreli, C. Giménez-Saiz, C.J. Gómez-García, P. Deplano, M.L. Mercuri, A. Serpe, L. Pilia, C. Faulmann, E. Canadell, Inorg. Chem. 46 (2007) 4446.
[50] I. Castro, M.L. Calatayud, F. Lloret, J. Sletten, M. Julve, J. Chem. Soc., Dalton Trans. (2002) 2397.
[51] N. Robertson, K. Awaga, S. Parsons, A. Kobayashi, A.E. Underhill, Adv. Mater. Opt. Electron. 8 (1998) 93.
[52] K. Awaga, T. Okuno, Y. Maruyama, A. Kobayashi, H. Kobayashi, S. Schenk, A.E. Underhill, Inorg. Chem. 33 (1994) 5598.
[53] M.L. Mercuri, P. Deplano, L. Leoni, J.A. Schlueter, U. Geiser, H.H. Wang, A.M. Kini, J.L. Manson, C. Gómez-García, E. Coronado, M.H. Whangbo, J. Mater. Chem. 12 (2002) 3570.
[54] L. Pilia, C. Faulmann, I. Malfant, V. Collière, M.L. Mercuri, P. Deplano, P. Cassoux, Acta Cryst. C 58 (2002) 240.
[55] Y. Kosaka, H.M. Yamamoto, A. Nakao, M. Tamura, R. Kato, J. Am. Chem. Soc. 129 (2007) 3054.
[56] H. Hiraga, H. Miyasaka, K. Nakata, T. Kajiwara, S. Takaishi, Y. Oshima, H. Nojiri, M. Yamashita, Inorg. Chem. 46 (2007) 9661.
[57] (a) H. Miyasaka, K. Nakata, L. Lecren, C. Coulon, Y. Nakazawa, T. Fujisaki, K. Sugiura, M. Yamashita, R. Clérac, J. Am. Chem. Soc. 128 (2006) 3770;
(b) H. Miyasaka, K. Nakata, K. Sugiura, M. Yamashita, R. Clérac, Angew. Chem., Int. Ed. 43 (2004) 707.

[58] (a) L. Lecren, W. Wernsdorfer, Y.-G. Li, O. Roubeau, H. Miyasaka, R. Clérac, J. Am. Chem. Soc. 127 (2005) 11311;
(b) L. Lecren, W. Wernsdorfer, Y.-G. Li, A. Vindigni, H. Miyasaka, R. Clérac, J. Am. Chem. Soc. 129 (2007) 5045.
[59] M.M. Ahmad, D.J. Turner, A.E. Underhill, Phys. Rev. B 29 (1984) 4796.
[60] (a) D. Gatteschi, R. Sessoli, J. Villain, Molecular Nanomagnets, Oxford University Press, Oxford, UK, 2006;
(b) H. Miyasaka, R. Clérac, Bull. Chem. Soc. Jpn. 78 (2005) 1725.